RSC Advances

Fabrication and characterization of high efficiency and stable Ag3PO4/TiO2 nanowire array heterostructure photoelectrodes for the degradation of methyl orange under visible light irradiation

Journal:	*RSC Advances*
Manuscript ID:	RA-ART-04-2015-006477.R2
Article Type:	Paper
Date Submitted by the Author:	18-May-2015

Complete List of Authors:	Jin, Bei; Lingnan Normal University, School of Chemistry and Chemical Engineering Zhou, Xiaosong; Lingnan Normal University, School of Chemistry and Chemical Engineering Luo, Jin; Lingnan Normal University, School of Chemistry and Chemical Engineering Xu, Xuyao; Lingnan Normal University, School of Chemistry and Chemical Engineering Ma, Lin; Lingnan Normal University, School of Chemistry and Chemical Engineering Huang, Dongyan; Lingnan Normal University, School of Chemistry and Chemical Engineering Shao, Zilun; Lingnan Normal University, School of Chemistry and Chemical Engineering Luo, Zhihui; Yulin Normal University, College of Chemistry and Material

RSC Advances

ARTICLE

Fabrication and characterization of high efficiency and stable Ag_3PO_4/TiO_2 nanowire array heterostructure photoelectrodes for the degradation of methyl orange under visible light irradiation †

Received 00th January 2015,
Accepted 00th January 2015

DOI: 10.1039/x0xx00000x

www.rsc.org/

Bei Jin,[a,c] Xiaosong Zhou,[a,]* Jin Luo,[a] Xuyao Xu,[a] Lin Ma,[a]Dongyan Huang,[a] Zilun Shao,[a] Zhihui Luo[b,]*

Ag_3PO_4/TiO_2 nanowire arrays (ATNWs) heterostructure photoelectrodes were prapared by a sequential chemical bath deposition. The structure and optical properties of the ATNWs were characterized by scanning electron microscopy, high-resolution transmission electron microscopy, X-ray diffraction, X-ray photoelectron spectroscopy, UV-Vis diffuse reflectance spectroscopy, photoluminescence spectroscopy and electrochemical techniques. The photocatalytic activity of the ATNWs was evaluated by photocatalytic degradation methyl orange (MO) under visible light irradiation (λ > 400 nm). The results showed that Ag_3PO_4 nanoparticles were successfully formed on the surface of the TiO_2 nanowires (NWs) causing no damage to the ordered structure of the nanowires. The p-type Ag_3PO_4 nanoparticles deposited on the n-type TiO_2 NWs could promote the transfer of photo-generated holes, which inhibited the recombination of electrons and holes effectively, leading to a significant increase in the lifetime of the charge carriers. Moreover, the ATNWs show much higher photocatalytic activity and stable than that of the pure TiO_2 NWs for the photocatalytic degradation MO. The enhanced photocatalytic activity could be attributed to the visible-light photocatalytic activity of Ag_3PO_4 and the heterostructure between Ag_3PO_4 and TiO_2.

Introduction

Well-ordered arrays of one-dimensional semiconductors have attracted much interest in the last decade as electrode architectures for optoelectronic applications. Recently, one-dimensional (1D) TiO_2 nanostructured materials such as nanowires, nanotubes, and nanorods, offering direct pathways for photogenerated electron transfer, possess advantages such as facile charge transport along the longitudinal dimensions, low electron-hole recombination rates, manifested superior photovoltaic and superhydrophilicity performance.[1] Several studies indicated that 1D TiO_2 nanowire arrays had improved properties compared to any other form of titania for photocatalysis,[2] hydrogen generation from water splitting, [3] solar cells,[4] lithium ion batteries[5] and water photo-oxidation.[6]

However, TiO_2 is a wide band gap energy semiconductor, active only under UV light irradiation. Because only a small fraction (ca. 4%) of solar radiation is in the ultraviolet region and visible light is far more abundant (ca. 45%),[7] it is one of the key objectives in the field of material science research to develop visible light active photocatalysts for solar energy conversion. In addition, the low efficiency of electron-hole separation limits the practical application of TiO_2 in photoelectrochemical and photocatalytic processes.[8] To overcome these problems, many modified approaches have been reported.[9]

Recently, Ye and co-workers have reported a breakthrough in using Ag_3PO_4 semiconductor as an active visible light driven photocatalyst for photodecomposition of organic compounds. [10] They have reported that the activity of Ag_3PO_4 is significantly higher than that of currently known visible light photocatalysts, e.g., $BiVO_4$ or N-doped TiO_2. However, Ag_3PO_4 nanoparticles suffer from stability issues in practical applications because they can photochemically decompose if no sacrificial reagent is involved.[10] Yao et al. reported the improved activity of the Ag_3PO_4/TiO_2 heterostructured photocatalyst for the degradation of dyes under visible light irradiation, which is attributed to the increased surface area and enhanced absorption of dyes.[11] Chen and co-workers have reported that $Ag/Ag_3PO_4/TiO_2$ heterostructure photoelectrodes for efficient decomposition of 2-chlorophenol under visible light irradiation. [12]

[a] School of Chemistry and Chemical Engineering, Institute of Physical Chemistry, and Development Center for New Materials Engineering & Technology in Universities of Guangdong, Lingnan Normal University, Zhanjiang 524048, China.Tel/Fax: +86-759-3183205; E-mail: zxs801213@163.com
[b] Guangxi Key Laboratory of Agricultural Products Processing (Cultivation Base), Guangxi Colleges and Universities Key Laboratory for Efficient Use of Agricultural Resources in the Southeast of Guangxi, College of Chemistry and Material, Yulin Normal University, Yulin, Guangxi 537000, China. E-mail:Lzhui_1980@163.com.
[c] Engineering Research Center of Starch and Vegetable Protein Processing, Ministry of Education，South China University of Technology, Guangzhou 510640, China.
† Footnotes relating to the title and/or authors should appear here.
Electronic Supplementary Information (ESI) available: [details of any supplementary information available should be included here]. See DOI: 10.1039/x0xx00000x

Herein, we reported p-type Ag_3PO_4 modified with highly ordered n-type TiO_2 nanowire arrays. The visible light photocatalytic activity of the Ag_3PO_4/TiO_2 heterostructure photoelectrodes was evaluated by the degradation of MO.

Experimental

Materials synthesis

The unique Ag_3PO_4/TiO_2 nanowire arrays heterostructure photoelectrodes on Ti-foil substrate were synthesized via a two-step deposition growth process, and the preparation process is shown in Fig. 1. A cleaned Ti sheet (99%) with thickness of 0.1 mm is placed against the wall of a 40 ml Teflon-lined stainless steel autoclave filled with 30 mL of 1.0 M NaOH in aqueous solution. Then, the sealed autoclave was put in an electric oven at 220 °C for 12 h. After cooled naturally to room temperature, the titanium foil was immersed in 0.5 M HCl solution for 3 h to replace Na^+ with H^+, rendering $H_2Ti_2O_5 \bullet H_2O$ nanowire arrays on Ti foil. Then, the Ti foil was washed with deionized water and absolute ethanol for several times, then dried at 60 °C for 12 h. The TiO_2 nanowire arrays were obtained after heat treatment in a tube furnace at 550 °C for 3 h in air with a ramping rate of 2 ºC/min.

The Ag_3PO_4 nanoparticles were deposited onto the crystallized TiO_2 nanowires by a sequential chemical bath deposition method.[13] First, the TiO_2 NWs electrode was immersed in an aqueous solution containing 0.10 M $AgNO_3$ solution for 15 min. It was then transferred to the next beaker containing 0.03 M NaH_2PO_4 solution and kept in there for 5 min. Finally, the electrode sample was rinsed with DI water. This preparation procedure was repeated for a number of times. The composites obtained were dried under vacuum at a temperature of 333 K for 12 h. The as-prepared samples were denoted ATNWs-X (X denotes the deposition times) .

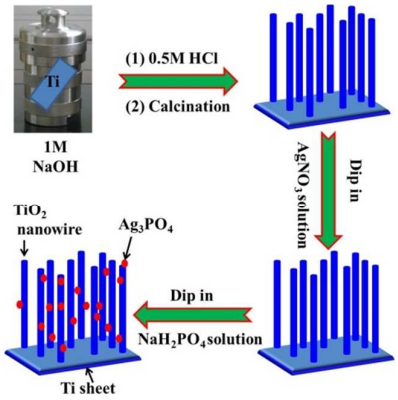

Fig. 1 The preparation of the Ag_3PO_4/TiO_2 NWs.

Materials characterization

X-ray diffraction (XRD) patterns of the as-prepared samples were recorded on an X-ray diffractometer (D/max-IIIA, Japan) using Cu K_a radiation. The surface morphology of as-prepared samples was examined by a scanning electron microscopy (SEM) (LEO1530VP, LEO Company) and a transmission electron microscope (TEM, JEOL, JEM2100). The UV-Vis light absorption spectra of as-prepared samples were obtained from a Hitachi UV-3010 spectrophotometer equipped with an integrating sphere assembly and using the diffuse reflection method and $BaSO_4$ as a reference to measure all the samples. The each of the chemical nature elements in the Ag_3PO_4/TiO_2 has been studied using X-ray photoelectron spectroscopy (XPS) in Krato Axis Ultra DLD spectrometer. The binding energy was referenced to C 1s line at 284.6 eV for calibration. Photoluminescence (PL) spectra were measured on an F-7000 Fluorescence spectrohpotometer (Hitachi, Japan).

Photochemical test of Ag_3PO_4/TiO_2 NWs

Photocurrent measurements were carried out in a standard electrodes photoelectrochemical cell by an electrochemical workstation (CV-27, BAS). The as-prepared samples, platinum-gauze and Ag/AgCl were used as working, counter and reference electrode, respectively. A sodium sulfate solution (0.5 M) is used as electrolyte. The light for the photocurrent was the filtered light (λ>400 nm, 150 mW·cm^{-2}) from a PLS-SXE 300UV Xe lamp.

The photocatalytic activity was measured in a XPAII reactor. The samples (0.8×2 cm^2) were immersed in 10 ml quartz test tubes containing 4 ml of methyl orange dye (MO, 10 mg·L^{-1}) in the dark for 1 h to achieve adsorption equilibrium before irradiation. After that, the visible light (λ>400 nm) photocatalytic experiments were conducted different times. The remaining dye concentrations in the reaction solution were determined using the U3010 spectrophotometer. The air were continuously passed in the whole decomposing process. The degradation ratio of MO can be calculated by:

$$X\% = (C_0 - C)/C_0 \times 100\% \quad (1)$$

where C_0 is the absorbance of original MO solution and C is theabsorbance of the MO solution after visible light irradiation.

According to the Langmuir–Hinshelwood kinetics model, thephotocatalytic process of MO can be expressed as the following apparent pseudo-first-order kinetics equation:[14]

$$\ln(C_0/C) = K_{app}t \quad (2)$$

Results and discussion

SEM observation shown in Fig. 2a has revealed high the average diameter of the highly ordered, well aligned pure TiO_2 nanowires, the length is about 5 μm and the diameter is around 30 nm. The SEM and TEM images of the TiO_2 NWs after the incorporation of Ag_3PO_4 nanoparticles are displayed in Fig. 2a and 2c. A more precise size distribution of Ag_3PO_4 nanoparticles throughout the TiO_2 nanowire surface could be observed from Fig. 2b and 2c, with a diameter of approximately 10 nm. It is note worthy that the TiO_2 nanowires still have a high level of orientation and have not damaged. Fig. 2d shows high magnification TEM images of Ag_3PO_4/TiO_2 NWs.The observed lattice fringes of 0.351 nm in the image (Fig. 2d) correspond to the (101) plane of anatase (JPCDS No.21-1272),[15] suggesting that the side walls of the

TiO_2 NWs are well crystallized. The observed lattice spacings of 0.269 nm, seen beside the nanowires, correspond to the (210) planes of Ag_3PO_4 (JPCDS No.06-0505),[12] respectively. These results confirmed that Ag_3PO_4 nanoparticles have been successfully deposited onto the TiO_2 NWs arrays.

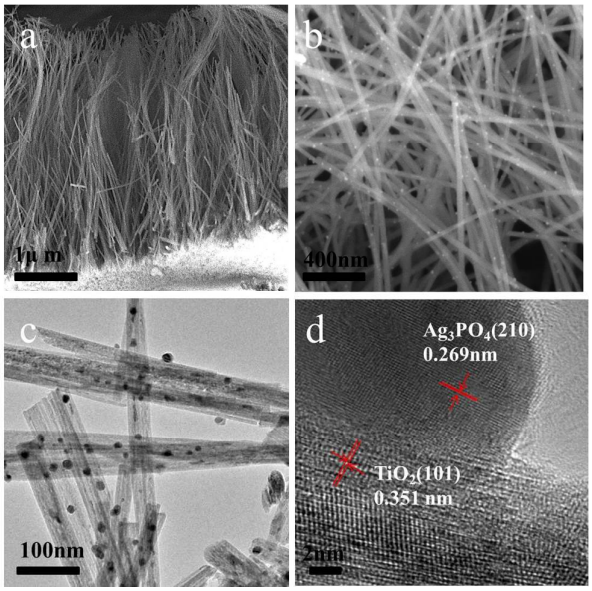

Fig. 2 SEM images of (a) TiO_2 NWs and (b) Ag_3PO_4/TiO_2 NWs, (c) TEM images of Ag_3PO_4/TiO_2 NWs and (d) HRTEM images of Ag_3PO_4/TiO_2 NWs.

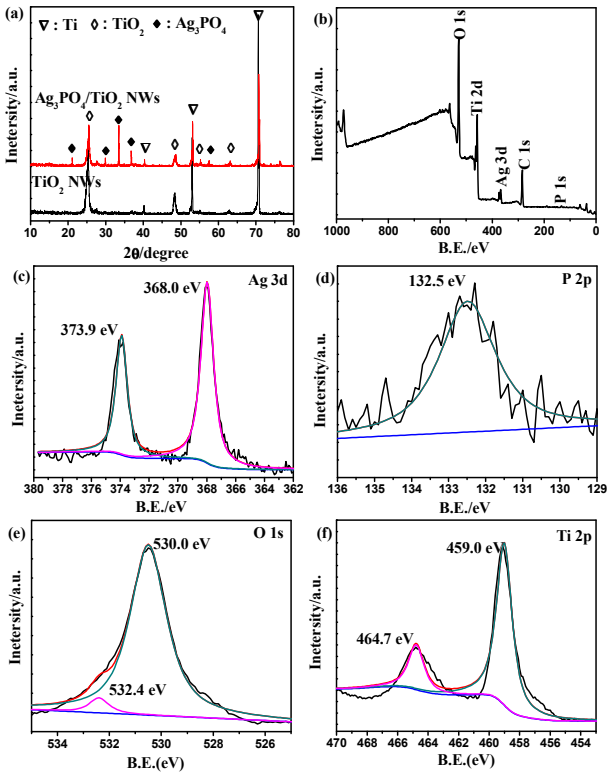

Fig. 3 (a) XRD patterns of the prepared TiO_2 NWs and Ag_3PO_4/TiO_2 NWs ; (b)-(f) XPS spectrum of Ag_3PO_4/TiO_2 NWs:(b) survey spectrum; (c) Ag 3d; (d) P 2p; (e) O 1s; (f) Ti 2p.

Fig. 3a shows the XRD patterns of the TiO_2 NWs and Ag_3PO_4/TiO_2 NWs. The pattern of the TiO_2 NWs is in good agreement with those of the Ti metal phase (JCPDS No. 05-0682) and anatase phase of TiO_2 (JCPDS No.21-1272)(Fig. 3a).[15] XRD results of the Ag_3PO_4/TiO_2 NWs reveals peaks at 2θ values of 20.9°, 29.7°, 33.3°, 36.9° and 55.0°(Fig. 3a) . These peaks can be indexed to the (110), (200), (210), (211) and (320) crystal planes of cubic Ag_3PO_4 (JCPDS No. 06-0505).[12] These results farther prove that Ag_3PO_4 nanoparticles have been successfully deposited onto the surface of the TiO_2 NWs. The high intensity of the peaks suggests that the Ag_3PO_4 nanoparticles actually have the crystalline structure as expected from the HRTEM images.

The elemental composition and chemical status of the as-prepared sample Ag_3PO_4/TiO_2 NWs were further analyzed by XPS (Fig. 3b-3f). The peaks corresponding to Ti, Ag, P and O were documented (Fig. 3b). The detailed spectra for Ag3d are shown in Fig. 3c. Two bands at 368.0 and 373.9 eV are observed and can be ascribed to the Ag $3d_{5/2}$ and Ag $3d_{3/2}$ binding energies, respectively, which can be attributed to the Ag^+ ions of Ag_3PO_4.[12] The binding energy of P 2p coming from the Ag_3PO_4 is 132.5 eV (Fig. 3d).[16]The XPS spectra of O 1s of the Ag_3PO_4/TiO_2 NWs were fitted tow peaks (Fig. 3e).The major peak at 530.0 eV is attributed to lattice oxygen, whereas a weak peak at 532.4 eV is due to the presence of surface hydroxyl groups.[17] It is found that the peaks of Ti $2p_{3/2}$ and Ti $2p_{1/2}$ are located at 459.0 and 464.7 eV, respectively (Fig. 3f). These peaks can be assigned to Ti^{4+} ions of TiO_2.[18]

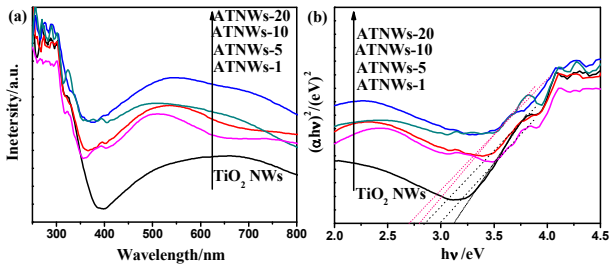

Fig. 4 (a) UV-Vis absorption spectra, and (b) Kubelka–Munk transformed reflectance spectra and estimated opticalabsorption bandgap of the as-prepared samples. The band gapenergy of as-prepared samples can be calculated from UV–Vis diffuse reflectance spectra, according to the equation: $\alpha h\nu \sim (h\nu - E_g)^2/h\nu$, in which α, ν, and E_g are the absorption coefficient, light frequency and energy band gap (at wave vector $k = 0$) of the semiconductor, respectively. [19a]

The UV-Vis diffuse refiection spectra of pure TiO_2 NWs and Ag_3PO_4/TiO_2 NWs are displayed in Fig. 4. The UV-Vis spectrum of the pure TiO_2 NWs sample indicates that it absorbs sunlight with a wavelength less than 390 nm (Fig. 4a), corresponding to

3.17 eV of band gap energy (Fig. 4b). Ag_3PO_4/TiO_2 NWs show a red shift in their absorption bands, and a strong photoabsorption in the wavelength region of 400-800 nm was obtained, which is attributed to the characteristic absorption of Ag_3PO_4 on TiO_2 NWs surface. The absorption intensity of the Ag_3PO_4/TiO_2 heterostructure composites was increased with the increasing amount of Ag_3PO_4 in reaction system.This feature of UV-Vis light absorption properties of the prepared Ag_3PO_4/TiO_2 photocatalyst suggests that the heterostructured Ag_3PO_4/TiO_2 NWs could be used for visible light photocatalytic reactions.

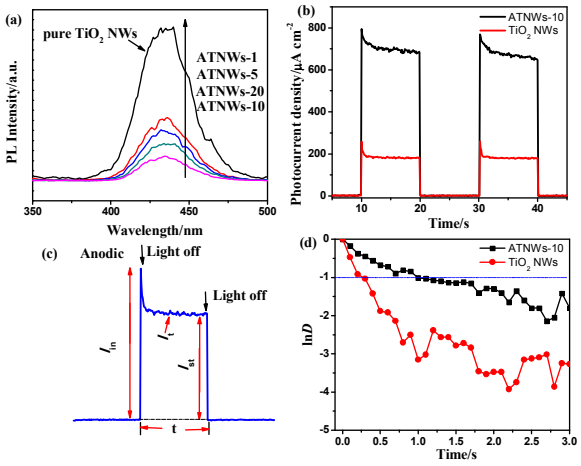

Fig. 5 (a) PL spectra of the as-prepared samples; (b-d) Anodic photocurrent dynamics of photoelectrodes at an applied bias 0.23V versus Ag|AgCl. (c) The scheme for the calculation of the transient dynamics is constant. (d) Anodic transient dynamics under AM 1.5G full-spectrum solar light with 150 $mW{\cdot}cm^{-2}$.

In order to investigate the effect of the Ag_3PO_4 modification, photoluminescence spectra analysis was applied to reveal the migration, transfer and recombination processes of photogenerated electron-hole pairs in composite samples. Fig. 5a shows the PL spectra for pure TiO_2 NWs and Ag_3PO_4/TiO_2 NWs with an excitation wavelength of 325 nm. As shown in Fig. 5a, the main emission peak is centered at about 435 nm for the pure TiO_2 NWs, which can be attributed to the band-band PL phenomenon with the energy of light approximately equal to the band gap energy of TiO_2. The PL intensity of the Ag_3PO_4/TiO_2 NWs was much lower than that of the TiO_2 NWs, indicating that the deposition of pure TiO_2 NWs has improved the charge separation effectively.

The photocurrent response measurement was carried out under visible light irradiation to investigate the photo-induced charge separation efficiency of Ag_3PO_4/TiO_2 NWs with deposition 10 times and pure TiO_2 NWs (Fig. 5b). It is clearly that the maximum photocurrent of ATNWs-10 increases about 3.5 times than that of pure TiO_2 NWs.To quantitatively determine the charge recombination behaviour, a normalized parameter (D) is introduced:

$$D=(I_t-I_{st})/(I_{in}-I_{st}) \quad (3)$$

where I_t, I_{st} and I_{in} are the time-dependent, steady-state and initial photocurrent, respectively, as shown in Fig. 5c.[19] The transient time constant (τ) is defined as the time when $\ln D=-1$ in the normalized plots of $\ln D \sim t$ (Fig. 5d), which reflects the general behaviour of charge recombination and lifetime of the charge carriers. τ was estimated to be 1.02 s for ATNMs-10 under 150 $mW{\cdot}cm^{-2}$ of visible light, which was 3.3 times than that of pure TiO_2 NWs (0.31 s), indicating the suppressed charge recombination.[20]

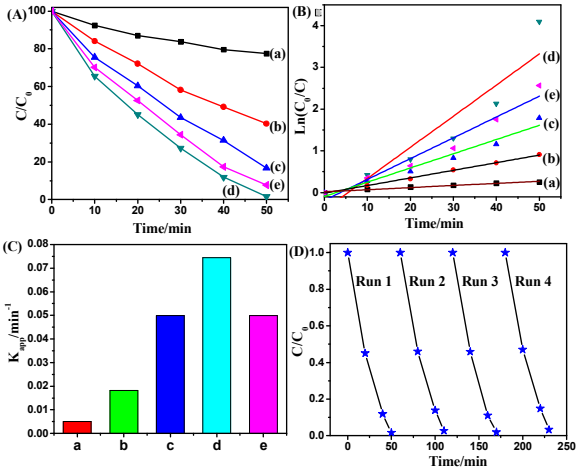

Fig. 6 (A) photocatalytic degradation of MO under visible light irradiation, (B) linear transform $\ln(C_0/C)$ of the kinetic curves of MO degradation, (C) the apparent pseudo-first-order rate constant k_{app} with different catalysts, (D) photocatalytic degradation of MO with ATNWs-10 for 4 runs : (a) pure TiO_2 NWs; (b) ATNWs-1; (c)ATNWs-5; (d) ATNWs-10; (e) ATNWs-20.

Fig. 6 presents a comparison of the pure TiO_2 NWs and all the synthesised Ag_3PO_4/TiO_2 NWs coupling samples. As can be seen from this figure, the Ag_3PO_4 content has a significant infiuence on the photocatalytic activity of pure TiO_2 NWs during the 50 min under visible light irradiation. From Fig. 6A, it can be seen that the photocatalytic degradation MO of pure TiO_2 NWs was 22.48%, however, when the time of deposited Ag_3PO_4 was increased to 10 times, the photocatalytic degradation MO reached the highest value of 98.33%. In this regard, the photocatalytic activity of sample ATNWs-10 exceeds that of pure TiO_2 NWs by a factor of 4.3. Fig. 6B shows that there is a linear relationship between $\ln C_0/C$ and t, confirming that the photodegradation reaction is indeed pseudo-first-order. According to Eq. (2) and Fig. 6C shows the apparent pseudo-first-order rate constant k_{app} with different catalysts. k_{app} of the photodegradation of MO are 0.0050, 0.0182, 0.0340, 0.0745 and 0.0498 min^{-1} for pure TiO_2 NWs, ATNWs-1, ATNWs-5, ATNWs-10, ATNWs-20, respectively. Obviously, an optimal degradation performance of MO was found for ATNWs-10. Increase loading amounts of Ag_3PO_4 to TiO_2 resulted in the decrease of photocatalytic activity of the photocatalyst composite, which is due to the aggregation of

Ag_3PO_4 particles.[11]The present results also showing that a suitable loading content of Ag_3PO_4 is crucial for optimizing the photocatalytic activity of Ag_3PO_4/TiO_2 NWs.

The stability of a photocatalyst is one of the important parameters for its usefulness. To study the stability of the Ag_3PO_4/TiO_2 NWs photocatalyst, used Ag_3PO_4/TiO_2 NWs were collected and reused in four successive MO degradation experiments. These experiments were carried out by adding used ATNWs-10 photocatalysts to fresh MO solutions with the same concentration, the results are shown in Fig. 6D. As no obvious decrease of degradation is observed after four runs, indicated that the Ag_3PO_4/TiO_2 NWs were outstanding stable during the photocatalytic reaction.

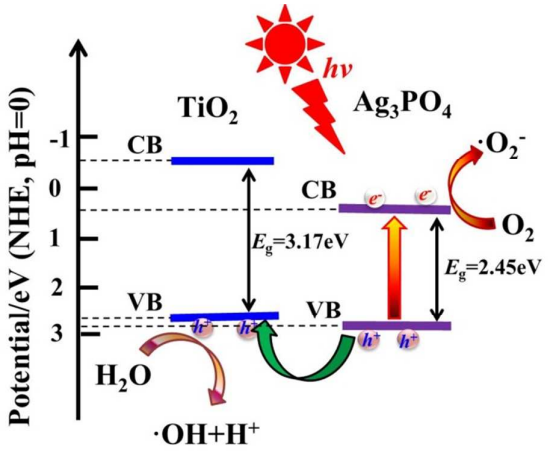

Fig. 7 Schematic illustration of the charge separation and transformationin the Ag_3PO_4/TiO_2 NWs system under visible light irradiation.

On the basis of the above results, a photocatalytic mechanism of the Ag_3PO_4/TiO_2 under visible-light irradiation can be proposed (Fig. 7). Because conduction band (CB) and valence band (VB) of Ag_3PO_4 are +0.45 eV *vs.* NHE and +2.9 eV *vs.* NHE, respectively.[8b] These potentials of both CB and VB of Ag_3PO_4 are more positive than those of TiO_2 (CB: -0.47eV *vs.* NHE, VB: +2.7 eV *vs.* NHE).[21] Under visible light irradiation, Ag_3PO_4 absorbs photons generate photo-generated electrons (e^-) and photo-generated holes (h^+) (Eq.(4)). Photon-generated holes in an Ag_3PO_4 particle quickly transfer to a VB of TiO_2 NWs (Eq.(5)), cause the oxidation of H_2O to ·OH (Eq.(6)). On the other hand, photo-generated electrons migrate to the surface of an Ag_3PO_4 nanoparticle, and then adsorbed O_2 to yield O_2^- (Eq.(7)). Highly oxidative species, such as ·OH, O_2^- and holes are produced, which then react with the MO, leading to methyl orange oxidation of inorganic small molecule, such as CO_2, H_2O, etc (Eq.(8)). Therefore, the efficient photocatalytic degradation of MO can smoothly proceed. The process is described as follows:

$$Ag_3PO_4 + hv \rightarrow Ag_3PO_4\,(e^-) + Ag_3PO_4\,(h^+) \quad (4)$$

$$Ag_3PO_4\,(h^+) \rightarrow TiO_2\,(h^+) \quad (5)$$

$$TiO_2\,(h^+) + H_2O \rightarrow \cdot OH + H^+ \quad (6)$$

$$Ag_3PO_4\,(e^-) + O_2 \rightarrow O_2^- \quad (7)$$

$$\cdot OH, O_2^-, h^+ + MO \rightarrow CO_2 + H_2O + \text{other inorganic molecules} \quad (8).$$

Conclusions

In this work, we have successfully prepared Ag_3PO_4/TiO_2 NWs heterostucture photoelectrodes by using a sequential chemical bath deposition. The incorporation of Ag_3PO_4 nanoparticles onto TiO_2 NWs extended the absorption spectrum of the TiO2 NWs significantly into visible light region. The photoelectrochemical performance of the Ag_3PO_4/TiO_2 NWs indicated that the Ag_3PO_4 nanoparticles on the surface of TiO_2 NWs, leading to a significant increase in the photocurrent density and a more effective separation of photo-generated electron-hole pairs. More significantly, the Ag_3PO_4/TiO_2 heterostructure photoelectrodes possess much higher photocatalytic activity than that of the pure TiO_2 NWs for the degradation of MO under visible light irradiation. Consequently, the TiO_2 heterostructure photoelectrodes described herein may be used in a wide range of applications including photocatalysis and solar cells.

Acknowledgements

This research was supported by Guangdong Natural Science Foundation (S2013040013755), Colleges and Universities in Guangdong Province Science and Technology Innovation Project (2013KJCX0123), Zhanjiang Science and Technology Research Projects (No. 2013B01152), the Open Project Program of Process of Starch and Vegetable Protein Engineering Research Center of Ministry of Education (2013-ERC-01), China Spark Program (2014GA780072), the Nature Science Foundation of Guangxi Province of China (2013GXNSFBA019045), the Program for Science and technology of Guangxi Education Department (2013YB194 and 201106LX521), the Startup Programs Foundation (G20130001 and G20130014).

Notes and references

1 a) J. M. Li, W. Wan,H. H. Zhou, J. J. Li, D. S. Xu, *Chem. Commun.* 2011, **47**, 3439-3441; b) S. Brutti, V. Gentili, H. Menard, B. Scrosati, P. G. Bruce, *Adv. Energy Mater.* 2012, **2**, 322-327.

2 a)X. Chen and S. S. Mao, *Chem. Rev.* 2007, **107**, 2891-2959; b)A. El Ruby Mohamed and S. Rohani, *Energy Environ. Sci.* 2011, **4**, 1065-1086.

3 a) G. M. Wang, H. Y. Wang, Y. C. Ling, Y. C. Tang, X. Y. Yang, R. C. Fitzmorris, C. C. Wang, J. Z. Zhang, Y. Li, *Nano Lett.* 2011, **11**, 3026-3033; b) X. Cao, G. Tian, Y. Chen, J. Zhou, W. Zhou, C. G. Tian and H. G. Fu. *J. Mater. Chem. A* 2014, **2**, 4366-4374.

4 a)J. Y. Liao, B. X. Lei, H. Y. Chen, D. B. Kuang, C. Y. Su, *Energy Environ. Sci.* 2012, **5**, 5750-5757; b) X. Sheng, D. He, J. Yang, K. Zhu, X. J. Feng, *Nano Lett.* 2014, **14**, 1848-1852.

5 a) J.Y. Liao, D. Higgins, G. Lui, V. Chabot, X. C. Xiao, Z. W. Chen, *Nano Lett.* 2013, **13**, 5467-5473; b)X. Hou, X. Wang, B.

Liu, Q. Wang, Z. Wang, D. Chen and G. Shen, *ChemElectroChem* 2014, **1**, 108-115.
6 S. Hoang, S. P. Berglund, N. T. Hahn, A. J. Bard, C. Buddie Mullins, *J. Am. Chem. Soc.* 2012, **134** , 3659-3662.
7 X. Chen, S. Shen, L. Guo, S. Mao, *Chem. Rev.* 2010, **110**,6503-6570.
8 a) P. Zhang, C. Shao, Z. Zhang, M. Zhang, J. Mu, Z. Guo, Y. Sun and Y. Liu, *J. Mater. Chem.* 2011, **21**, 17746-17753; b) H. Chen, M. Shen, R. Chen, K. Dai and T. Peng, *Environ. Technol.* 2011, **32**, 1515-1522.
9 K. Dai, T. Peng, H. Chen, J. Liu and L. Zan, *Environ. Sci. Technol.* 2009, **43**, 1540-1545; b)M. Shen, X. Zhang, K. Dai, H. Chen and T. Peng, *CrystEngComm* 2013, **15**, 1146–1152.
10 a)Z. Yi, J. Ye, N. Kikugawa, T. Kako, S. Ouyang, H. S. Williams, H. Yang, J. Cao, W. Luo, Z. Li, Y. Liu and R. L. Withers, Nat. Mater. 2010, 9, 559-564; b)Y. Bi, S. Ouyang, N. Umezawa, J. Cao and J. Ye, *J. Am. Chem. Soc.* 2011, **133**, 6490-6492; c) Y. Bi, S. Ouyang, J. Cao and J. Ye, *Phys. Chem. Chem. Phys.* 2011, **13**, 10071-11075.
11 W. Yao, B. Zhang, C Huang, C. Ma, X. Song, Q. Xu, *J. Mater. Chem.* 2012, **22**, 4050-4055.
12 W. Teng, X. Li, Q. Zhao, G. H. Chen, *J. Mater. Chem. A* 2013, **1**, 9060–9068.
13 G. Larramona, C. Choné, A. Jacob, D. Sakakura, B. Delatouche, D. Péré, X. Cieren, M. Nagino and R. Bayón, *Chem. Mater.* 2006, **18**, 1688-1696.
14 K. Dai, L. Lu, Q. Liu, G. Zhu, Q. Liu, *Catal. Commun.* 2014, **43**, 202-206.
15 F. Sun, W. Zhou, G. Tian, K. Pan, X. Miao, Y. Li, G. Zhang,T. Li,H. Fu, *ChemCatChem* 2012, **4**, 844 – 850.
16 Y. P. Liu, L. Fang, H. D. Lu, Y. W. Li, C. Z. Hu, H. G. Yu, *Appl. Catal. B: Environ.* 2012, **115-116**, 245-252.
17 a) D. Seo, J. C. Park and H. Song, *J. Am. Chem. Soc.*, 2006, **128**, 14863-14870; b) G. Dai, J. Yu and G. Liu, *J. Phys. Chem. C* 2011, **115**, 7339- 7346.
18 a)X. B. Chen, C. Burda , *J. Phys. Chem.B* 2004, **108**, 15446-15449; b)X. S. Zhou, B. Jin, L. D. Li, F. Peng, H. J. Wang, H. Yu and Y. P. Fang, *J. Mater. Chem.* **2012**, 22, 17900-17905.
19 a) K. Dai, L. Lu, C. Liang, Q. Liu, G. Zhu, *Appl. Catal. B: Environ*. 2014, **156–157**, 331–340; b) D. Tafalla, P. Salvador, R. M. Benito, *J. Electrochem. Soc.* 1990, **137**, 1810–1815.
20 a) N. L. Dmitruk, A. V. Korovin, I. B. Mamontova, *Sem. Sci. Tech.* 2009, **24**, 125011; b)J. T. Li, S. K. Cushing, P. Zheng, F. Meng, D. Chu, N.Q. Wu, *Nature Commun.* 2013, **4**,2651-2658.
21 a) L. Yang, S. Luo, Y. Li, Y. Xiao, Q. Kang and Q. Cai, *Environ. Sci. Technol.* 2010, **44**, 7641-7646; b) C. Liu, H. Chen, K. Dai, A. Xue, H. Chen and Q. Huang, *Mater. Res. Bull.* 2013, **48**, 1499-1505.

Graphical Abstract

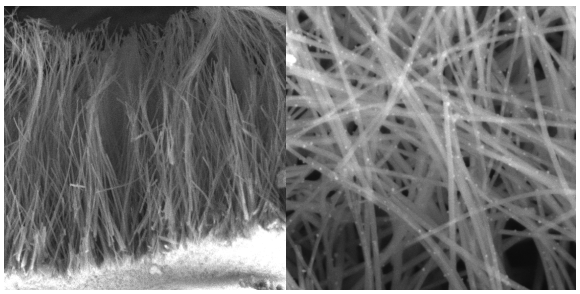

Ag_3PO_4/TiO_2 nanowire array heterostructure photoelectrodes with excellent photocatalytic and photoelectrochemical properties under visible light are prepared.